





RESEARCH ARTICLE

Stenoparib, an inhibitor of cellular poly (ADP-ribose) polymerases (PARPs), blocks *in vitro* replication of SARS-CoV-2 variants

Katherine E. Zarn¹ , Sierra A. Jaramillo¹ , Anthony R. Zapata¹, Nathan E. Stone¹, Ashley N. Jones¹, Haley E. Nunnally¹, Erik W. Settles^{1,2}, Ken Ng¹, Paul S. Keim^{1,2}, Steen Knudsen³ , Patricia M. Nuijten⁴, Aloys S. L. Tijms⁴, Christopher T. French^{1,2,5*} 

1 Pathogen and Microbiome Institute, Northern Arizona University, Flagstaff, Arizona, United States of America, **2** Department of Biological Sciences, Northern Arizona University, Flagstaff, Arizona, United States of America, **3** Allarity Therapeutics Europe, Hørsholm, Denmark, **4** Viroclinics-DDL, Rotterdam, The Netherlands, **5** COVID-19 Testing Service Center, Pathogen and Microbiome Institute, Northern Arizona University, Flagstaff, Arizona, United States of America

 These authors contributed equally to this work.

* ctfrench@nau.edu



OPEN ACCESS

Citation: Zarn KE, Jaramillo SA, Zapata AR, Stone NE, Jones AN, Nunnally HE, et al. (2022) Stenoparib, an inhibitor of cellular poly (ADP-ribose) polymerases (PARPs), blocks *in vitro* replication of SARS-CoV-2 variants. PLoS ONE 17(9): e0272916. <https://doi.org/10.1371/journal.pone.0272916>

Editor: Philippe A. Gallay, Scripps Research Institute, UNITED STATES

Received: March 11, 2022

Accepted: July 28, 2022

Published: September 14, 2022

Copyright: © 2022 Zarn et al. This is an open access article distributed under the terms of the [Creative Commons Attribution License](https://creativecommons.org/licenses/by/4.0/), which permits unrestricted use, distribution, and reproduction in any medium, provided the original author and source are credited.

Data Availability Statement: All relevant data are within the paper and its [Supporting information](#).

Funding: This research was supported by a grant from The Flinn Foundation awarded to PSK (grant # 2304; <https://flinn.org/>), the Cowden Endowment for Microbiology (a private endowment through the Northern Arizona University Foundation), and an Arizona Board of Regents Technology and Research Initiative Fund award to PSK and CTF (<https://www.azleg.gov/ars/15/01648.htm>). Core

Abstract

We recently published a preliminary assessment of the activity of a poly (ADP-ribose) polymerase (PARP) inhibitor, stenoparib, also known as 2X-121, which inhibits viral replication by affecting pathways of the host. Here we show that stenoparib effectively inhibits a SARS-CoV-2 wild type (BavPat1/2020) strain and four additional variant strains; *alpha* (B.1.1.7), *beta* (B.1.351), *delta* (B.1.617.2) and *gamma* (P.1) *in vitro*, with 50% effective concentration (EC₅₀) estimates of 4.1 μM, 8.5 μM, 24.1 μM, 8.2 μM and 13.6 μM, respectively. A separate experiment focusing on a combination of 10 μM stenoparib and 0.5 μM remdesivir, an antiviral drug, resulted in over 80% inhibition of the *alpha* variant, which is substantially greater than the effect achieved with either drug alone, suggesting at least additive effects from combining the different mechanisms of activity of stenoparib and remdesivir.

Introduction

As of June 2022, the coronavirus disease (COVID-19) pandemic, caused by SARS-CoV-2, has caused over 534 million infections and over 6.3 million deaths worldwide [1]. Although protective vaccines are available, the pandemic continues, and both old and new SARS-CoV-2 variants exhibit varying degrees of disease severity and resistance to vaccination. Additional effective therapeutics are urgently needed. Here we describe the antiviral activity of a small molecule, stenoparib, an inhibitor of mammalian poly (ADP-ribose) polymerases (PARPs). We show that stenoparib effectively inhibits replication of SARS-CoV-2 wild-type (*wt*) and variant strains *in vitro*.

SARS-CoV-2 has undergone adaptation and mutation since the beginning of the COVID-19 pandemic, resulting in new variants of the virus. Only two antiviral drugs, remdesivir and molnupiravir, or treatment with monoclonal antibodies, have been approved by the United States Food and Drug Administration as COVID-19 therapies under the Emergency Use

experiments were supported by service fees paid by Allarity Therapeutics. SK received funding in the form of salary from the commercial organization Allarity Therapeutics. PMN and ASLT received funding in the form of salary from the commercial organization Viroclinics-DDL. The funders had no additional role in study design, data collection and analysis, decision to publish, or preparation of the manuscript. The specific roles of these authors are articulated in the 'author contributions' section.

Competing interests: SK is employed by and holds a financial interest in Allarity Therapeutics, which stands to potentially benefit from these results. PMN and ASLT are employed by Viroclinics-DDL. This does not alter our adherence to PLOS ONE policies on sharing data and materials. There are no patents, products in development or marketed products associated with this research to declare.

Authorization [2, 3]. Remdesivir and molnupiravir are nucleoside analogs that affect the activity of the RNA-dependent RNA polymerase (RdRp). After incorporation into viral RNA, remdesivir stalls the RdRp during elongation [4], while molnupiravir results in the incorporation of mutations that can be functionally deleterious [5].

We recently published a study on the activity of a poly (ADP-ribose) polymerase (PARP) inhibitor, stenoparib, also known as 2X-121, which inhibits viral replication by affecting pathways of the host [6] as opposed to targeting viral replication. ADP-ribosylation (ADPR) pathways may have either anti- or pro-viral properties, and their importance in host-virus interactions is becoming increasingly recognized [7]. Unlike remdesivir, which inhibits viral replication downstream of entry into the cell, stenoparib inhibits virus entry and post-entry processes [6]. Stenoparib inhibited the SARS-CoV-2 USA-WA1/2020 virus and the HCoV-NL63 human seasonal respiratory coronavirus *in vitro*, exhibiting dose-dependent suppression of virus multiplication and cell-cell spread in cell culture [6]. Stenoparib exhibits a unique dual activity against the PARP1, 2 and PARP5a, 5b (tankyrase 1, 2) enzymes, which are important intermediates in the Wnt/ β -catenin immune checkpoint [8, 9]. As a host-targeting therapeutic that does not directly select for resistance in viruses, we hypothesize that stenoparib should be able to inhibit all SARS-CoV-2 variant strains.

Materials and methods

Cell culture

For the ViroSpot reduction assays (performed in The Netherlands), the antiviral activity of stenoparib (catalog # S8419, Selleckchem Chemicals, Radnor, PA, USA) on SARS-CoV-2 was assessed *in vitro* using Vero E6 *Cercopithecus aethiops* kidney cells (catalog # CRL-1586, ATCC, Manassas, VA, USA, acquired September 2020) maintained in Dulbecco's Modified Eagle Medium (DMEM; catalog # BE12-733F, Lonza, Basel, Switzerland) supplemented with 2 mM L-glutamine (catalog # BE17-605E, Lonza, Basel, Switzerland), 100 U/ml penicillin and 100 μ g/mL streptomycin (catalog # DE17-602E, Lonza, Basel, Switzerland), and 3% fetal bovine serum (FBS; catalog # FBS-12A, Capricorn Scientific, Ebsdorfergrund, Germany).

For the cytotoxicity assays and plaque assays (performed in the United States), the cytotoxicity and antiviral activity of stenoparib on SARS-CoV-2 was assessed *in vitro* using Vero E6 *Cercopithecus aethiops* kidney cells (catalog # CRL-1586, ATCC, Manassas, VA, USA, acquired September 2020) maintained in Eagle's Minimum Essential Medium (EMEM; catalog # 30-2003, ATCC, Manassas, VA, USA) supplemented with 2% or 10% FBS, 100 U/mL penicillin and 100 μ g/mL streptomycin (catalog # P0781, Sigma Aldrich, St. Louis, MO, USA), 0.01 M HEPES solution (catalog # H0887, Sigma Aldrich, St. Louis, MO, USA), 1 mM sodium pyruvate (catalog # 11360070, ThermoFisher Scientific, Waltham, MA, USA), and 1 \times non-essential amino acids solution (catalog # SH3023801, Fisher Scientific, Waltham, MA, USA).

ViroSpot reduction assay

The activities of stenoparib and remdesivir (catalog # 30354, Cayman Chemical Company, Ann Arbor, MI, USA) were assessed in a BSL3 facility against a *wt* SARS-CoV-2 strain (BavPat1/2020), and four additional SARS-CoV-2 variants of concern; *alpha* (B.1.1.7), *beta* (B.1.351) *delta* (B.1.617.2), and *gamma* (P1), hereafter referred to using Greek nomenclature (Table 1). We performed ten, serial 2-fold dilutions of compound, mixed with 100 plaque-forming units (pfu) of virus, and added the mixture to 80% confluent Vero E6 cells growing in multi-well plates. The Vero E6 cells were fixed 20 hours (h) after infection and stained with a SARS-CoV/SARS-CoV-2 Nucleocapsid monoclonal antibody (Sino Biological, Wayne, PA, USA) followed by a horseradish peroxidase (HRP)-labeled Goat anti-Mouse IgG (catalog # G-21040,

Table 1. SARS-CoV-2 variants used in ViroSpot reduction and plaque assays to evaluate antiviral properties of stenoparib and remdesivir.

Variant	Pango lineage	Strain	Isolate	Source
<i>wt</i>	-	BavPat1/2020	Germany	European Virus Archive–GLOBAL; 026V-03883
<i>alpha</i>	B.1.1.7	hCoV-19/USA/CA_CDC_5574/2020	California, USA	BEI Resources; NR-54011
<i>beta</i>	B.1.351	hCoV-19/USA/MD-HP01542/2021	Maryland, USA	BEI Resources; NR-55282
<i>delta</i>	B.1.617.2	hCoV-19/USA/PHC658/2021	Tennessee, USA	BEI Resources; NR-55611
<i>gamma</i>	P.1	Isolate hCoV-19/Japan/TY7-503/2021	Japan	BEI Resources; NR-54982

The *wt*, *alpha*, *beta*, *delta*, and *gamma* strains were used in the ViroSpot reduction assay. The *alpha* strain was used in the plaque assays. The *delta* strain carries an ORF7a deletion which may have the potential to impact virulence [17]. The following reagents were obtained through BEI Resources, NIAID, NIH: SARS-Related Coronavirus 2, Isolate USA/CA_CDC_5574/2020, NR-54011, deposited by the Centers for Disease Control and Prevention; SARS-Related Coronavirus 2, Isolate hCoV-19/USA/MD-HP01542/2021 (Lineage B.1.351), in *Homo sapiens* Lung Adenocarcinoma (Calu-3) Cells, NR-55282, contributed by Andrew S. Pekosz; SARS-Related Coronavirus 2, Isolate hCoV-19/USA/PHC658/2021 (Lineage B.1.617.2; *Delta* Variant), NR-55611, contributed by Dr. Richard Webby and Dr. Anami Patel; and SARS-Related Coronavirus 2, Isolate hCoV-19/Japan/TY7-503/2021 (Brazil P.1), NR-54982, contributed by National Institute of Infectious Diseases.

<https://doi.org/10.1371/journal.pone.0272916.t001>

ThermoFisher, Waltham, MA, USA) and TrueBlue Peroxidase Substrate (catalog # 5510–0030, Seracare, Milford, MA, USA). Spots were counted using a CTL ImmunoSpot Image Analyzer (Cleveland, OH, USA) as previously described [10]. Percent inhibition was calculated as percent of the well surface area covered by virus-positive immunostaining, and was normalized by taking the average fraction of the wells that showed positive staining compared to the control wells with the highest positive staining [10]. The EC₅₀ values were approximated and compared in a pair-wise fashion using package ‘drc 3.0–1’ in R version 4.1.1 [11–13]. We calculated means and standard deviations using package ‘matrixStats’ version 0.62.0 and ‘psych’ version 2.2.5 in R version 4.1.1 [13–15]. Mean normalized percent inhibition and dose-response curves were plotted using Hill coefficient, minimum, maximum, and EC₅₀ parameter estimates from package ‘drc’ version 3.0–1 and the Hill equation in R version 4.1.1 [11–13, 16].

Plaque assay

Vero E6 cells were infected with the SARS-CoV-2 *alpha* variant in a BSL3 facility using a multiplicity of infection (MOI) of 0.1, and the activity of stenoparib was assessed with and without remdesivir using a plaque reduction assay. Following viral infection and treatment with stenoparib and/or remdesivir, cells were overlaid with low melting point agarose (catalog # 1613112, BioRad, Hercules, CA, USA), fixed at 120 h post infection with 4.0% paraformaldehyde (catalog # AAJ19943K2, Fisher Scientific, Waltham, MA, USA), stained with crystal violet (catalog # V5265, Sigma Aldrich, St. Louis, MO, USA), and plaques were manually counted. We used Welch’s Two Sample t-tests in R version 4.1.1 [13] to perform pairwise t-tests between the untreated wells and wells under all other treatment conditions. Standard deviations and error bars were plotted using packages ‘matrixStats’ and ‘psych’ in R version 4.1.1 [13–15].

Cytotoxicity assay

Cytotoxicity was measured using the Promega CytoTox 96 Non-Radioactive Cytotoxicity Assay (catalog # G1780, Promega, Madison, WI, USA) in 50 μ L reactions and 96-well format

(catalog # 161093, Thermo Scientific, Waltham, MA, USA) according to the manufacturer's protocol. The assay was measured using a BioTeK Synergy HT plate reader (model # 7091000, BioTek, Winooski, VT, USA) set at 490 nm wavelength. Vero E6 cells were assessed for cytotoxicity at 5 days post-treatment. Percent cytotoxicity was calculated by dividing the experimental LDH release at 490 nm wavelength (OD_{490}) by the maximum LDH release control (lysis) and multiplying by 100. Means and standard deviations were calculated and plotted using packages 'matrixStats' and 'psych' in R version 4.1.1[13–15].

Results

We explored the activity of stenoparib against a *wt* SARS-CoV-2 strain and four variant strains *alpha*, *beta*, *delta*, and *gamma* (Table 1). Inhibition of virus replication by stenoparib was dose-dependent, with 50% effective concentration (EC_{50}) estimates ranging from 4.1 μ M to 24.1 μ M across the five virus strains tested (Fig 1A). Interestingly, the EC_{50} estimate for stenoparib and the *beta* variant (24.1 μ M) was 2.8- to 5.8-fold higher than for the *wt*, *alpha*, and *delta* variants, which were 4.1 μ M, ($p = 1.19 \times 10^{-4}$); 8.5 μ M, ($p = 7.96 \times 10^{-9}$); and 8.2 μ M, ($p = 0.06$; S1 and S2 Figs). Similarly, the EC_{50} estimate for stenoparib against the *gamma* variant (13.6 μ M) was lower than for the *beta* variant (24.1 μ M), however this difference was not statistically significant ($p = 0.22$; S1 and S2 Figs). An analogous phenomenon was noted for remdesivir. The *beta* EC_{50} estimate (9.9 μ M) for remdesivir was 2.1- to 4.3-fold higher than for the *wt*, *alpha*, *delta*, and *gamma* variants; 3.8 μ M, ($p = 2.76 \times 10^{-5}$); 4.7 μ M, ($p = 2.05 \times 10^{-11}$); 2.3 μ M, ($p = 4.97 \times 10^{-3}$); and 4.1 μ M ($p = 2.32 \times 10^{-4}$), respectively (Fig 1B, S1 and S2 Figs). The standard deviation around the percent inhibition estimates was high for the *beta* variant, however, so the dose-response correlation may not be precisely calculated in this case (Fig 1B). The ViroSpot experiment was conducted using technical quadruplicates, and infected and untreated cells were used as controls.

In an additional set of experiments, we focused on the SARS-CoV-2 *alpha* variant. Vero E6 cells were infected with the *alpha* variant using a multiplicity of infection of 0.1, and the activity of stenoparib was assessed with and without remdesivir using the plaque reduction assay.

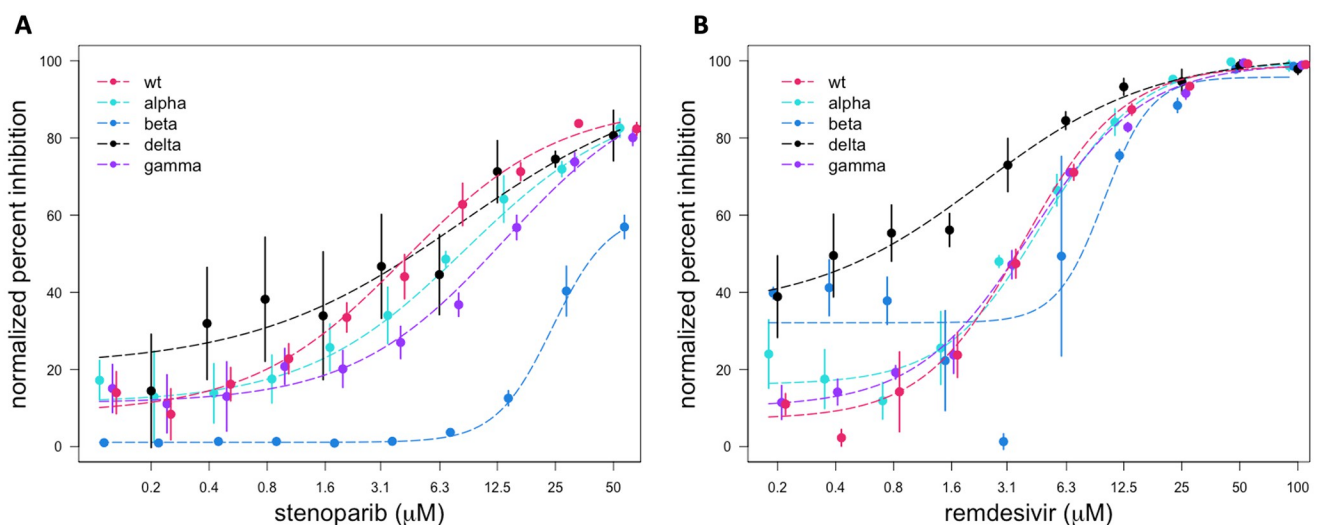


Fig 1. Dose-response curves for stenoparib and remdesivir on wild type SARS-CoV-2 and four variant SARS-CoV-2 strains. Normalized percent inhibition (Y-axis) of *wt* SARS-CoV-2 and variant strains *alpha*, *beta*, *delta*, and *gamma* in Vero E6 cells treated with (A) stenoparib or (B) remdesivir at the indicated concentrations (X-axis). Error bars are the standard deviation.

<https://doi.org/10.1371/journal.pone.0272916.g001>

Plaques are areas of dead or destroyed cells and appear as small, clear regions in an infected cell monolayer after fixation and staining with crystal violet. We combined 2.5, 5.0, and 10 μM doses of stenoparib with the previously reported EC_{50} of remdesivir (0.5 μM) [6]. The three control types were 1) infected and untreated cells, 2) uninfected and untreated cells, and 3) infected cells treated with a combination of camostat mesylate and aloxistatin (E64d) (combination hereafter referred to as Camostat-E64d, or 'CE'), which are protease inhibitors that prevent Spike (S) protein cleavage and virus entry into the cell [12].

As shown in Fig 2A and 2B, neither 10 μM stenoparib nor 0.5 μM remdesivir achieved greater than a 50% reduction in plaquing efficiency compared to the infected, untreated cells. When combined, however, plaque formation was reduced by over 80% compared to infected, untreated cells. This reduction was superior to what was achievable with stenoparib ($p = 3.03 \times 10^{-5}$) or remdesivir ($p = 1.99 \times 10^{-4}$) alone at these doses. Notably, cytotoxicity remained near baseline levels (Fig 2C). The cytotoxicity experiments were run in triplicate and cells were treated with CE, dimethylsulfoxide (DMSO), lysis buffer, or left untreated (no compound) as controls. When combined, the activity of two or more drugs with different mechanisms of activity may synergize, with the potential benefit of reducing individual doses of each drug and minimizing undesirable side effects in the patient.

Discussion

According to a recent report, the *beta* variant appears to exhibit a significantly reduced eclipse period (length of time between initial infection and the production of virus by a cell) and more rapid replication *in vitro* compared to the *alpha* variant [17]. This could explain the relatively higher stenoparib and remdesivir EC_{50} estimates for the *beta* variant. In addition to numerous changes to the S protein, the *beta* variant carries some unique mutations in the N protein and in the Nsp3 polyprotein (ORF1a) that are not found in the other variants [18], and may be involved in viral degradation pathways including ADPR following infection [19]. Differential susceptibility to ADPR may be related to the altered replication kinetics of the *beta* variant, although verifying this requires further investigation.

In this study, the activity of remdesivir and stenoparib against SARS-CoV-2 was examined in Vero E6 African green monkey kidney cells, which are highly permissive to infection with SARS-CoV-2 [20]. Our previous stenoparib study utilized Vero E6 and Calu-3 human lung adenocarcinoma cells, which were less sensitive than Vero E6 to the toxic effects of stenoparib at higher concentrations and the extended incubation times (120 h) required for the plaque assay [6]. Host cell lines vary in their susceptibility to infection and in their response to treatment with antivirals. Additional studies using other host cell lineages, including primary respiratory epithelial cells, should be instructive regarding the efficacy of PARP inhibitors as host-targeting antiviral therapeutics.

Besides the known roles for the PARP1 and PARP2 enzymes in DNA repair [21, 22], members of the PARP family have numerous additional functions [23]. The 18 known human PARPs appear to differentially affect viral replication; some exhibit proviral activity and others exhibit antiviral roles [7, 24–28]. In coronavirus, the N protein is mono (ADP) ribosylated (MARylated) during infection. Stability of the N protein is critical for viral genome replication, translation, packaging, and modulation of the host cell cycle [29]. The N protein is the only ADPR target definitively identified in coronavirus thus far [24], and the prevalence of this modification across multiple coronavirus families suggests an important role in virus stability [24]. Despite this, the role of N protein MARylation, and of ADPR in general with regards to coronavirus stability, is not well characterized. Possibly ADPR has a role in regulating virus genome structure, like ADPR of histones or the adenovirus core proteins [30, 31]. While

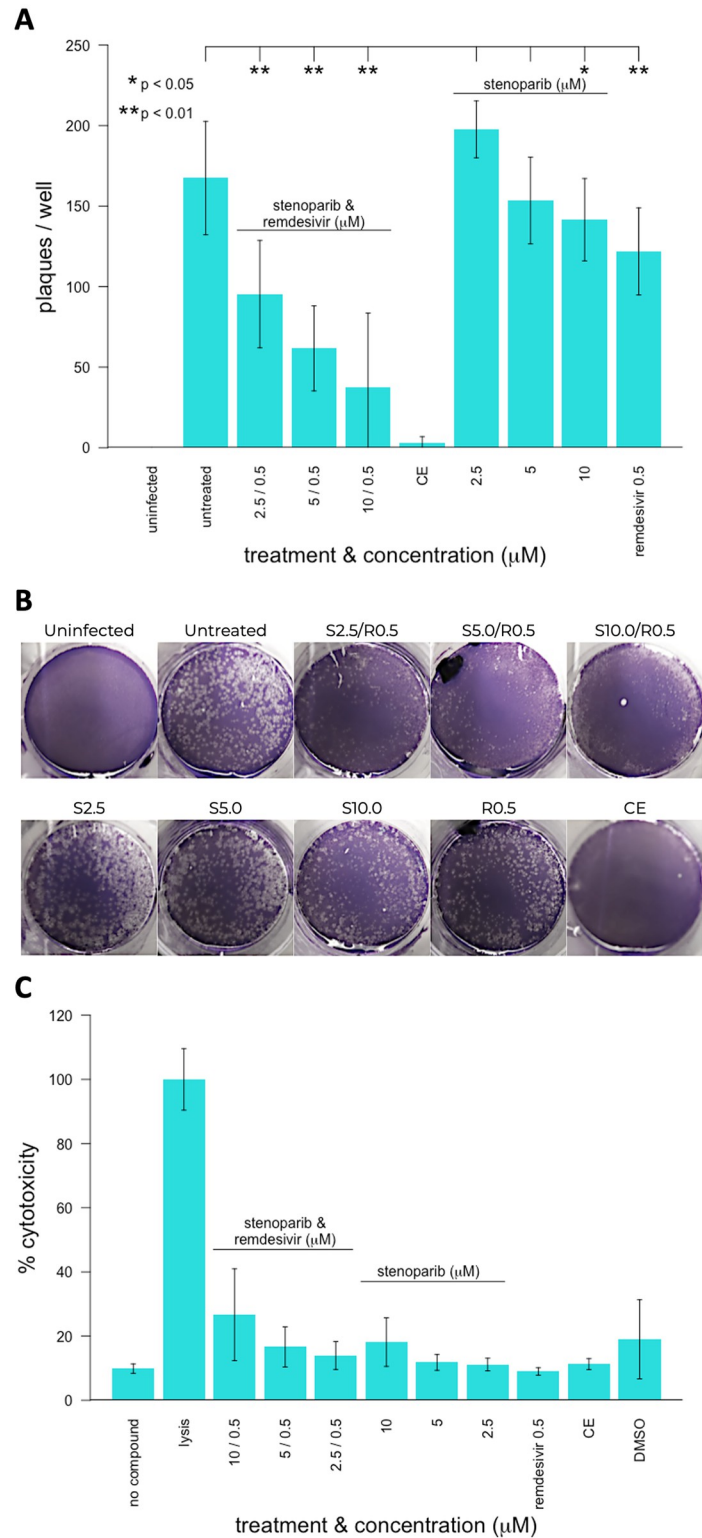


Fig 2. Activity of stenoparib and remdesivir on the *alpha* SARS-CoV-2 variant and cytotoxicity of stenoparib and remdesivir in Vero E6 cells. (A) Virus plaque assays. Vero E6 cells were infected for 2 hours with SARS-CoV-2 *alpha* variant, washed, and overlaid with low-melting temp agarose/MEM with or without stenoparib and/or remdesivir at the concentrations indicated. The cell monolayers were fixed with 4% paraformaldehyde and stained with 0.1% crystal violet prior to manual counting of plaques. The experiment was performed using technical triplicates and error bars

represent the standard deviation of three independent experiments. For pairwise comparisons to untreated cells, * indicates p-values less than 0.05 and ** indicates p-values less than 0.01. (B) Photographs of plaque assay plate wells after crystal violet staining. Labels indicate the concentrations of stenoparib or remdesivir. Abbreviations: S = stenoparib, R = remdesivir at the concentrations indicated (i.e. 2.5 / 0.5 = 2.5 μ M stenoparib, 0.5 μ M remdesivir). (C) Cytotoxicity measurements performed by the lactate dehydrogenase release assay (Promega Cytotox 96) 48 hours after infection. Inhibitors stenoparib or remdesivir were used at the indicated concentrations (X-axis). The assays were performed according to the manufacturer's recommendations. Results from drug treatments were normalized to the fraction of maximum cytotoxicity (% Cytotoxicity; Y-axis) achieved by detergent lysis of cells. The samples were processed in triplicate and error bars represent the standard deviation of five independent experiments.

<https://doi.org/10.1371/journal.pone.0272916.g002>

remdesivir and molnupiravir inhibit viral RNA replication, stenoparib likely acts through multiple targets. A combination of stenoparib and remdesivir or molnupiravir may be highly effective at inhibiting SARS-family coronaviruses including SARS-CoV-2.

Here, we showed that stenoparib is broadly inhibitory to SARS CoV-2, including emerging variants of concern. We expect these results to apply for additional, emergent variants as well, and recent preliminary data with stenoparib and the *omicron* variant supports this. A host-targeting therapeutic like stenoparib could be a significant benefit for COVID-19 patients as a standalone therapy, or as part of a combinatorial COVID-19 treatment strategy with an antiviral drug such as remdesivir or molnupiravir. Combinations of two or more drugs may lead to synergism through different mechanisms of action, which has the potential benefit of reducing individual doses of each drug and minimizing undesirable side effects.

Supporting information

S1 Fig. Stenoparib and remdesivir EC₅₀ estimates. Stenoparib (gold shading) and remdesivir (blue shading) EC₅₀ estimates for Vero E6 cells infected with SARS-CoV-2 *wt*, *alpha*, *beta*, *delta*, or *gamma* variants.
(TIF)

S2 Fig. P-values for SARS-CoV-2 variant pairwise comparisons of stenoparib and remdesivir EC₅₀ estimates. Stenoparib (above the diagonal, gold shading) and remdesivir (below the diagonal, blue shading) EC₅₀ pairwise comparisons for SARS-CoV-2 *wt*, *alpha*, *beta*, *delta*, or *gamma* variants.
(TIF)

S1 Dataset. Data from ViroSpot assays, plaque assays, and cytotoxicity assays.
(XLSX)

Author Contributions

Conceptualization: Erik W. Settles, Paul S. Keim, Steen Knudsen, Christopher T. French.

Data curation: Katherine E. Zarn.

Formal analysis: Katherine E. Zarn, Sierra A. Jaramillo, Christopher T. French.

Funding acquisition: Paul S. Keim, Steen Knudsen, Christopher T. French.

Investigation: Katherine E. Zarn, Sierra A. Jaramillo, Anthony R. Zapata, Ashley N. Jones, Haley E. Nunnally, Patricia M. Nuijten, Aloys S. L. Tijmsma.

Methodology: Nathan E. Stone, Christopher T. French.

Project administration: Paul S. Keim, Steen Knudsen, Aloys S. L. Tijmsma, Christopher T. French.

Resources: Paul S. Keim, Christopher T. French.

Supervision: Erik W. Settles, Paul S. Keim, Christopher T. French.

Visualization: Katherine E. Zarn, Ken Ng.

Writing – original draft: Christopher T. French.

Writing – review & editing: Katherine E. Zarn, Nathan E. Stone, Erik W. Settles, Paul S. Keim, Aloys S. L. Tijmsa, Christopher T. French.

References

1. WHO. 2021. <https://covid19.who.int/>. Accessed 15 June 2022.
2. National Center for Immunization and Respiratory Diseases (NCIRD), Division of Viral Diseases. Information for Clinicians on Investigational Therapeutics for Patients with COVID-19 Centers for Disease Control and Prevention. 2020. <https://www.cdc.gov/coronavirus/2019-ncov/hcp/therapeutic-options.html>
3. Beigel JH, Tomashek KM, Dodd LE, Mehta AK, Zingman BS, Kalil AC, et al. Remdesivir for the Treatment of Covid-19—Final Report. *The New England Journal of Medicine*. 2020; 383(19):1813–26. Epub 2020/05/24. <https://doi.org/10.1056/NEJMoa2007764> PMID: 32445440.
4. Kocic G, Hillen HS, Tegunov D, Dienemann C, Seitz F, Schmitzova J, et al. Mechanism of SARS-CoV-2 polymerase stalling by remdesivir. *Nat Commun*. 2021; 12(1):279. Epub 2021/01/14. <https://doi.org/10.1038/s41467-020-20542-0> PMID: 33436624.
5. Kabinger F, Stiller C, Schmitzova J, Dienemann C, Kocic G, Hillen HS, et al. Mechanism of molnupiravir-induced SARS-CoV-2 mutagenesis. *Nat Struct Mol Biol*. 2021; 28(9):740–6. Epub 2021/08/13. <https://doi.org/10.1038/s41594-021-00651-0> PMID: 34381216.
6. Stone NE, Jaramillo SA, Jones AN, Vazquez AJ, Martz M, Versluis LM, et al. Stenoparib, an Inhibitor of Cellular Poly(ADP-Ribose) Polymerase, Blocks Replication of the SARS-CoV-2 and HCoV-NL63 Human Coronaviruses *In Vitro*. *mBio*. 2021; 12(1):e03495–20. <https://doi.org/10.1128/mBio.03495-20> PMID: 33468703
7. Kuny CV, Sullivan CS. Virus-Host Interactions and the ARTD/PARP Family of Enzymes. *PLOS Pathogens*. 2016; 12(3):e1005453. Epub 2016/03/25. <https://doi.org/10.1371/journal.ppat.1005453> PMID: 27010460.
8. McGonigle S, Chen Z, Wu J, Chang P, Kolber-Simonds D, Ackermann K, et al. E7449: A dual inhibitor of PARP1/2 and tankyrase1/2 inhibits growth of DNA repair deficient tumors and antagonizes Wnt signaling. *Oncotarget*. 2015; 6(38):41307–23. Epub 2015/10/30. <https://doi.org/10.18632/oncotarget.5846> PMID: 26513298.
9. Thorsell AG, Ekblad T, Karlberg T, Low M, Pinto AF, Tresaugues L, et al. Structural Basis for Potency and Promiscuity in Poly(ADP-ribose) Polymerase (PARP) and Tankyrase Inhibitors. *J Med Chem*. 2017; 60(4):1262–71. Epub 2016/12/22. <https://doi.org/10.1021/acs.jmedchem.6b00990> PMID: 28001384.
10. van Baalen CA, Jeeninga RE, Penders GH, van Gent B, van Beek R, Koopmans MP, et al. ViroSpot microneutralization assay for antigenic characterization of human influenza viruses. *Vaccine*. 2017; 35(1):46–52. Epub 2016/12/03. <https://doi.org/10.1016/j.vaccine.2016.11.060> PMID: 27899226.
11. Ritz C SJ. Package ‘drc’. Analysis of dose-response data is made available through a suite of flexible and versatile model fitting and after-fitting functions. <https://cran.r-project.org/web/packages/drc/drc.pdf>:CRAN; 2016.
12. Ritz C, Baty F, Streibig JC, Gerhard D. Dose-Response Analysis Using R. *PLOS ONE*. 2015; 10(12):e0146021. Epub 20151230. <https://doi.org/10.1371/journal.pone.0146021> PMID: 26717316.
13. R Core Team. R: A language and environment for statistical computing. R Foundation for Statistical Computing, Vienna, Austria 2018. <https://www.R-project.org/>.
14. Revelle W. psych: Procedures for Psychological, Psychometric, and Personality Research. R Package Version 1.0–95. Evanston, Illinois. 2013.
15. Bengtsson H. Henrik Bengtsson (2017). matrixStats: Functions that Apply to Rows and Columns of Matrices (and to Vectors). R package version 0.52.2. 2017.
16. Hill AV, Hill AV, Paganini-Hill A. The possible effects of the aggregation of the molecules of haemoglobin on its dissociation curves. *The Journal of Physiology*. 1910; 40:4–7.
17. Pyke AT, Nair N, van den Hurk AF, Burtonclay P, Nguyen S, Barcelon J, et al. Replication Kinetics of B.1.351 and B.1.1.7 SARS-CoV-2 Variants of Concern Including Assessment of a B.1.1.7 Mutant

- Carrying a Defective ORF7a Gene. *Viruses*. 2021; 13(6). Epub 2021/07/03. <https://doi.org/10.3390/v13061087> PMID: 34200386.
18. Hodcroft EB. CoVariants: SARS-CoV-2 Mutations and Variants of Interest 2021. <https://covariants.org/>.
 19. Lei J, Kusov Y, Hilgenfeld R. Nsp3 of coronaviruses: Structures and functions of a large multi-domain protein. *Antiviral Res*. 2018; 149:58–74. Epub 2017/11/13. <https://doi.org/10.1016/j.antiviral.2017.11.001> PMID: 29128390.
 20. Puray-Chavez M, LaPak KM, Schrank TP, Elliott JL, Bhatt DP, Agajanian MJ, et al. Systematic analysis of SARS-CoV-2 infection of an ACE2-negative human airway cell. *Cell Rep*. 2021; 36(2):109364. Epub 20210623. <https://doi.org/10.1016/j.celrep.2021.109364> PMID: 34214467.
 21. Dziadkowiec KN, Gasiorowska E, Nowak-Markwitz E, Jankowska A. PARP inhibitors: review of mechanisms of action and BRCA1/2 mutation targeting. *Prz Menopauzalny*. 2016; 15(4):215–9. <https://doi.org/10.5114/pm.2016.65667> PMID: 28250726.
 22. Ame JC, Rolli V, Schreiber V, Niedergang C, Apiou F, Decker P, et al. PARP-2, A novel mammalian DNA damage-dependent poly(ADP-ribose) polymerase. *The Journal of biological chemistry*. 1999; 274(25):17860–8. Epub 1999/06/11. <https://doi.org/10.1074/jbc.274.25.17860> PMID: 10364231.
 23. Gupte R, Liu Z, Kraus WL. PARPs and ADP-ribosylation: recent advances linking molecular functions to biological outcomes. *Genes & development*. 2017; 31(2):101–26. <https://doi.org/10.1101/gad.291518.116> PMID: 28202539.
 24. Grunewald ME, Fehr AR, Athmer J, Perlman S. The coronavirus nucleocapsid protein is ADP-ribosylated. *Virology*. 2018; 517:62–8. Epub 2017/12/05. <https://doi.org/10.1016/j.virol.2017.11.020> PMID: 29199039.
 25. Grunewald ME, Chen Y, Kuny C, Maejima T, Lease R, Ferraris D, et al. The coronavirus macrodomain is required to prevent PARP-mediated inhibition of virus replication and enhancement of IFN expression. *PLOS Pathogens*. 2019; 15(5):e1007756. Epub 2019/05/17. <https://doi.org/10.1371/journal.ppat.1007756> PMID: 31095648.
 26. Li L, Zhao H, Liu P, Li C, Quanquin N, Ji X, et al. PARP12 suppresses Zika virus infection through PARP-dependent degradation of NS1 and NS3 viral proteins. *Science Signaling*. 2018; 11(535): eaas9332. <https://doi.org/10.1126/scisignal.aas9332> PMID: 29921658.
 27. Atasheva S, Frolova EI, Frolov I. Interferon-stimulated poly(ADP-Ribose) polymerases are potent inhibitors of cellular translation and virus replication. *Journal of Virology*. 2014; 88(4):2116–30. Epub 2013/12/11. <https://doi.org/10.1128/JVI.03443-13> PMID: 24335297.
 28. Westera L, Jennings AM, Maamary J, Schwemmler M, Garcia-Sastre A, Bortz E. Poly-ADP Ribosyl Polymerase 1 (PARP1) Regulates Influenza A Virus Polymerase. *Adv Virol*. 2019; 2019:8512363. Epub 2019/04/25. <https://doi.org/10.1155/2019/8512363> PMID: 31015836.
 29. McBride R, van Zyl M, Fielding BC. The coronavirus nucleocapsid is a multifunctional protein. *Viruses*. 2014; 6(8):2991–3018. Epub 2014/08/12. <https://doi.org/10.3390/v6082991> PMID: 25105276.
 30. Déry CV, de Murcia G, Lamarre D, Morin N, Poirier GG, Weber J. Possible role of ADP-ribosylation of adenovirus core proteins in virus infection. *Virus Research*. 1986; 4(4):313–29. [https://doi.org/10.1016/0168-1702\(86\)90078-x](https://doi.org/10.1016/0168-1702(86)90078-x) PMID: 2941933
 31. Strickfaden H, McDonald D, Kruhlik MJ, Haince J-F, Th'ng JPH, Rouleau M, et al. Poly(ADP-ribosyl)ation-dependent Transient Chromatin Decondensation and Histone Displacement following Laser Microirradiation*. *Journal of Biological Chemistry*. 2016; 291(4):1789–802. <https://doi.org/10.1074/jbc.M115.694992> PMID: 26559976